

the beam pattern radiation in the horizontal plane. This type of beamforming is referred to as 2DBF, which is often combined with cell sectorization to exploit frequency reuse, reduce interference among users, and increase cell capacity. In this method, rather than adopting an omnidirectional antenna at the BS, each cell is divided into sectors (e.g., three sectors) and each sector is served by a directional antenna. The antenna that supports each sector is a one-dimensional array of antenna elements that provides a fan-shaped radiation pattern. These patterns have a wide beamwidth (e.g., 70°) in the horizontal or azimuth plane and a relatively narrow beamwidth (e.g., 10°) in the vertical or elevation plane (see Figure 1). The number of horizontal radiation patterns that can be produced in each sector depends on the number of antennas in that sector. If more than one antenna is placed in each sector, it is possible to form and direct multiple beams to different angles in the horizontal plane. Then, each of these patterns can support one user or a group of users in a specific direction.

BASICS OF 3DBF

As just mentioned, in 2DBF, the beam pattern is designed only in the horizontal plane. To utilize the vertical domain, antenna tilt can be considered in the vertical axis. The antenna tilting angle is defined as the angle between the horizontal plane and the boresight direction of the antenna pattern. To adjust the tilting angle of the antenna along the vertical axis, mechanical alignment of the antenna can be adopted. In fact, as depicted in Figure 2(a) (which represents mechanical tilt), some adjustable

brackets are used to change the tilting angle of the antenna. On the other hand, in some antennas, it is also possible to control the tilting angle electrically (which is called electrical tilt). As shown in Figure 2(b), electrical downtilting is realized by applying an overall phase shift to all antenna elements in the array [6].

An active antenna system (AAS) is a recent technology that helps in getting more control on antenna elements individually. In the AAS, each array element is integrated with a separate radio-frequency (RF) transceiver unit that provides remote control to the elements electronically. By employing AAS at the BS of cellular networks, the vertical radiation pattern can also be adjusted dynamically in each sector, and multiple elevation beams can also be generated to support multiple users or cover multiple regions. A design of 3DBF is achieved by appending this type of vertical beamforming and conventional horizontal beamforming [7].

Depending on the way that the antenna downtilt is changed, 3DBF can be classified into static 3DBF and dynamic 3DBF. The static 3DBF refers to a system where the antenna tilt at the BS is set to a fixed value according to some statistical metrics, e.g., the mean value of the vertical angles of users [7]. This method cannot be adapted to the changing location of the users, i.e., once the tilting angle is selected, it will remain unchanged. In contrast, the dynamic 3DBF is a technique that steers the BS antenna tilting angle instantaneously according to specific user locations. Thus, the mechanical tilt is considered a special case of the static 3DBF, since the tilting angle is determined by the long-term average sense. On the other hand, the dynamic 3DBF

HIGHER USER CAPACITY, LESS INTERCELL AND INTERSECTOR INTERFERENCE, HIGHER ENERGY EFFICIENCY, IMPROVED COVERAGE, AND INCREASED SPECTRAL EFFICIENCY ARE SOME OF THE ADVANTAGES OF 3DBF.

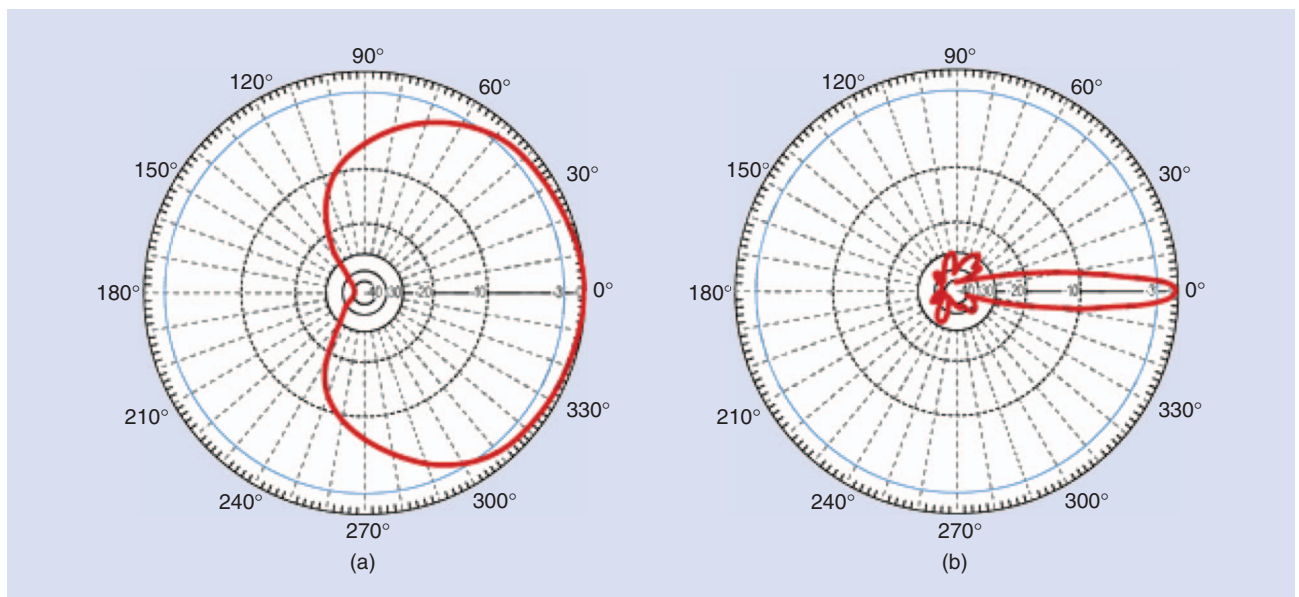


[FIG1] A typical radiation pattern of a BS antenna in (a) horizontal plane and (b) vertical plane.

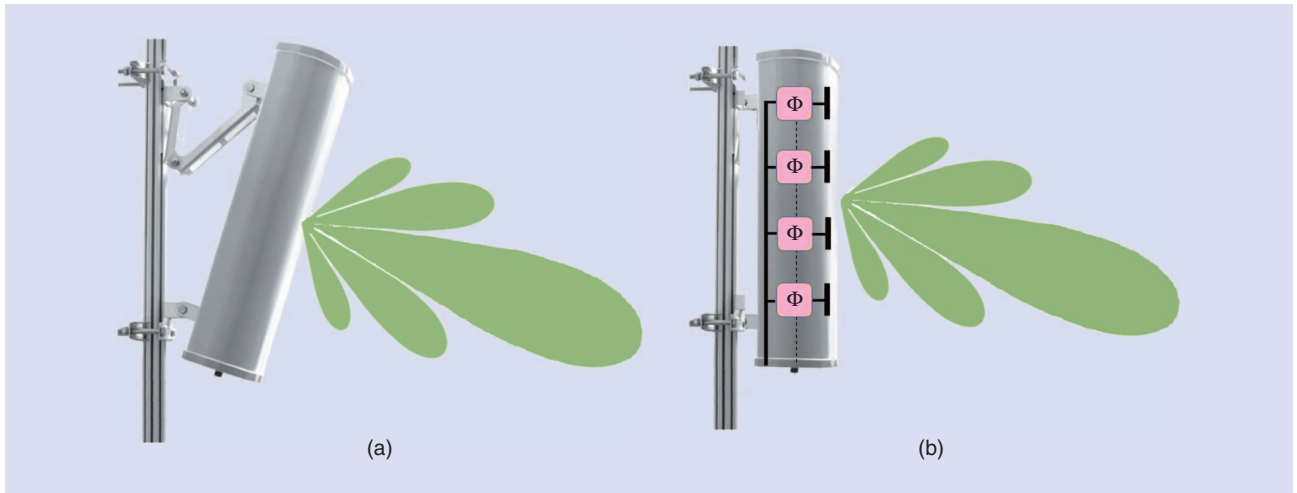


[FIG2] A comparison of different antenna downtilting methods: (a) mechanical tilting and (b) electrical tilting.

includes the electrical tilt as a special case. We can expect that the dynamic 3DBF offers additional degrees of freedom for performance optimization compared to the static 3DBF.

In comparison to the 2DBF, the 3DBF can provide improved capabilities on managing intercell interference in multicell scenarios. When vertical beamforming is applied, different powers can be allocated to the beam patterns that serve cell-edge and cell-center regions separately. This prevents extra power radiation to adjacent cells and decreases the intercell interference in the network. Thus, the 3DBF achieves a higher capacity gain compared to the 2DBF, and its performance gain will be confirmed in the “Simulation Results” section later.

The standardization of the 3DBF has been started in the Third Generation Partnership Project (3GPP) Release 12. In this release, the activities have been limited to a study of feasibility of the 3DBF and its potential gains. The 3DBF implementation is expected to begin at the end of 2015 or even later. It is also foreseen that enhancements to the specifications of the 3DBF will continue at the 3GPP Releases 14 and 15. Works on these two releases will probably start in 2016 and be finalized in 2020. We observe a similar trend in other technologies such as massive MIMO and small cells, which are currently examined in 4G networks and also introduced as promising technologies for 5G networks. In spite of the aforementioned advantages of the 3DBF, there are still some challenges with this technology that

need to be addressed. Some of these challenges include three-dimensional (3-D) channel modeling, the overhead related to channel state information (CSI) feedback in frequency division duplexing (FDD) scenarios, power control, antenna designs, and complexity of RF chains.

APPLICATIONS OF DYNAMIC AND STATIC 3DBF

Applying the dynamic 3DBF, a BS can direct the main lobe of the antenna beam to a specific user. As a consequence, the desired signal strength at the intended users is maximized. The 3DBF can also be used to suppress intercell interference in a multicell scenario by adjusting the antenna beams properly. By adopting coordination between neighboring cells, it is possible to achieve a tradeoff between the desired signal power at the intended users and the intercell interference level, and then a further performance improvement is expected.

On the other hand, the static 3DBF in a cellular network can be combined with cell sectorization, which also improves the network performance. As we see in Figure 3(a), the traditional sectorization method provides sectors that are formed along the tangential direction in the horizontal plane. However, as depicted in Figure 3(b), employing two tilting angles at each sector enables additional sectorization along the radial direction, which is called vertical sectorization. Splitting the cell into several sectors can utilize more frequency reuse and

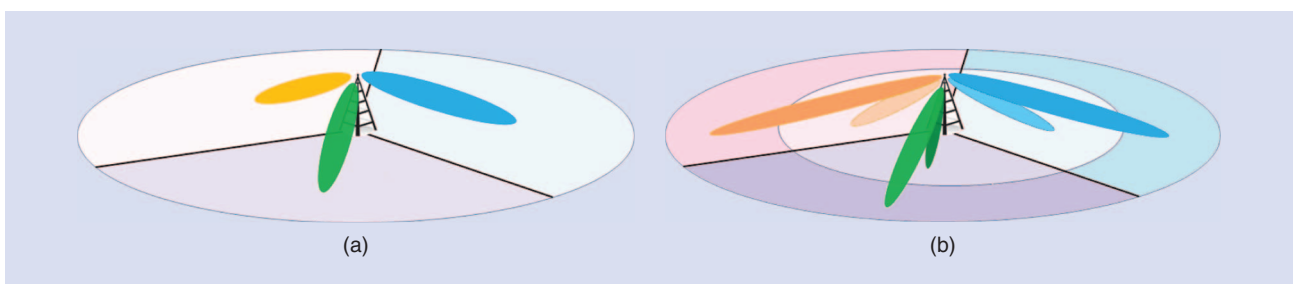


[FIG3] (a) Conventional sectorization. (b) Vertical sectorization.

significantly increase the network capacity. For example, a capacity gain (in terms of the mean throughput) of 70 and 140% can be achieved by moving from three sectors to six and 12 sectors, respectively [8]. Similar gains are also reported in the scenarios that employ vertical sectorization with 3DBF [9]. In addition, vertical sectorization by 3DBF provides more flexibility in traffic load balancing compared to the conventional sectorization by adaptively changing the number of sectors to serve variable traffic loads in the cell [10].

Another important issue in 3DBF is how to acquire CSI to design precoders at the BS. In time-division duplexing (TDD) systems, by exploiting channel reciprocity, CSI of the downlink is obtained from an estimate of the uplink. In FDD systems, the CSI is estimated by a user and then the BS obtains this information through feedback from the user to the BS. In this case, if the number of antenna elements at the BS increases, the feedback overhead is a challenging problem. Hence, in some precoding methods, precoding designs are based on partial or reduced-dimensional CSI [11]. In addition, another problem in TDD operation is the number of training symbols that need to be sent in each coherence block of transmission. This training overhead problem becomes more challenging if the number of users in the network increases [12], and these issues are still open problems in 3DBF.

REVISIT OF 3DBF IN OTHER AREAS

So far, we have discussed the advantages and challenges of 3DBF. It is interesting to note that although 3DBF is a relatively new topic in wireless cellular networks, its history can be traced back to the 1970s when some early methods were proposed for applying multiple elevation radiation beams in radar and underwater sonar systems. For example, in [13], which was published in 1978, the concept of the vertical beamforming was employed for an array of antennas or acoustic elements in synthetic aperture radar systems to increase the resolution of target detection. In this system, multiple contiguous elevation beams with different frequencies are adopted, which can be considered as frequency reuse in cellular networks.

Apart from radio communication systems, techniques similar to the 3DBF have been applied in other areas of signal processing. It is worth studying similarities between those application areas and cellular communication to gain insights on current challenges of 3DBF. One popular application of 3DBF can be found in imaging. Three-dimensional imaging is widely adopted in medical systems using ultrasound, microwave, and X-ray [14], and 3DBF can provide higher-resolution and image quality compared to the conventional methods. For example, in [15], an ultrasound imaging scheme employed 3DBF to synthesize a 3-D volume with a 16×16 planar receiving array and a 6×6 transmit array, and the 3DBF algorithm was decomposed into two simpler 2DBF processes. The idea of these works can be used in designing the antenna arrays and also adaptive beamforming and vertical sectorization methods for cellular systems.

Audio and speech processing is another major application area that has already adopted the 3DBF. In this case, the 3DBF

is utilized in a two-dimensional (2-D) or 3-D array of loudspeakers to focus sound radiation to a specific location. Similarly, an array of microphones and the 3DBF can be applied to receive sound from a desired direction in the 3-D space. For example, a moving person can be tracked while she/he speaks or a sound source can be localized in video conference applications [16]. In [17], a 3DBF technique was proposed to use a spherical array consisting of pressure microphones where different frequencies and wave propagation effects of audio and radio waves are taken into account. An example of such an array is illustrated in Figure 4. These configurations can provide inspiration for designing 3-D antenna arrays topologies for wireless communication. The scheme in [17] is based on a spherical harmonic decomposition of the sound field for acoustic applications and is capable of steering the beam pattern to any direction in the 3-D space without changing the shape of the pattern. This can also give ideas for designing beam patterns in the 3DBF with per-user beam steering, considering that modifying the antenna beam shape with the elevation and azimuth angles may increase interuser interference and affect the performance of the 3DBF in the network. These abundant prior works related to the 3DBF demonstrate that this technique has a strong connection to other signal processing areas. By exploiting these results already developed in other applications, a successful deployment of 3DBF in 5G systems can be made possible.

3-D WIRELESS CHANNEL MODELING

To evaluate the performance of the 3DBF in cellular systems, a proper 3-D channel model is required. In particular, the power spectral density of the received signals and the channel capacity are dependent on the adopted channel model. Similar to other multiple antenna technologies, a channel model for the 3DBF must accurately describe the spatial environment along with



[FIG4] A spherical array of loudspeakers (figure used with permission of [30]).

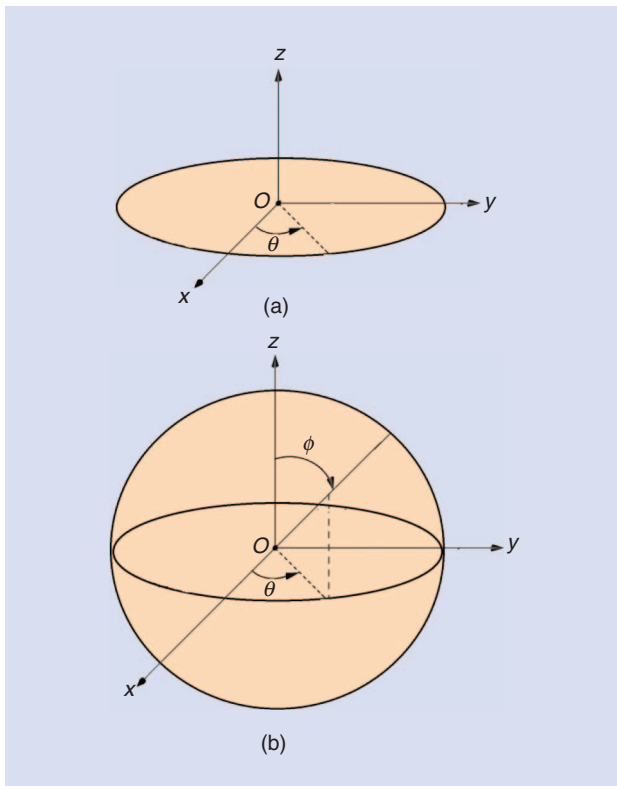


[FIG5] The (a) 2-D and (b) 3-D channel models.

time and frequency characteristics. To capture the spatial properties of 3DBF, we need two types of information: antenna configurations and the propagation field properties [18].

Most of the basic channel models in cellular networks are 2-D models. The 2-D models such as the 3GPP spatial channel model (SCM) [19] or International Telecommunications Union (ITU) double directional channel model [20] consider a distribution of scatterers only in the azimuth plane and do not take the elevation angle into account. For example, the widely used Clark's model [21] is also a 2-D model that assumes all signals received from uniform directions in the azimuth plane as shown Figure 5(a). However, some practical measurements in the urban environments show that up to 65% of energy is incident with elevation angles larger than 10° [22].

To improve the 2-D models, several studies have been conducted on 3-D channel models to include nonzero elevation angles and accurately evaluate the systems. For example, some works have been initiated by 3GPP to define the 3-D channel models for vertical beamforming in LTE [23]. One of the first research works on the statistical modeling of the 3-D fading channels was described in [24], which is an extension of Clark's 2-D model. In this model, the scatterers are assumed to be distributed in a cylinder around the receiver and, in fact, both azimuth and elevation angles of arrival are taken into account. Here, the azimuth angle is distributed uniformly in a circle, while the elevation angle has a nonuniform distribution. This model was later extended to a two-cylinder model in which both transmitter and receiver are

assumed to be placed inside two cylinders of scatterers. In a general case, the scatterers can exist inside a sphere around the receiver [as in Figure 5(b)].

One of the most popular 3-D channel models in literature is the WINNER channel model [25], which is an extension of a previous 3GPP 2-D SCM and 2-D ITU model. In addition to different elevation and azimuth angles, this model also includes other parameters such as the number of antennas, the vertical and horizontal radiation patterns, and dual-polarization transmissions. The model can accommodate the bandwidth of up to 100 MHz and carrier frequencies between 2 and 6 GHz. Most of the model's parameters are deduced from empirical measurements. More details about this model can be found in [25].

Although there are some 3-D models that can be used for current wireless networks, a complete and accurate 3-D channel model will be highly desirable for actual evaluation of the 3DBF and other novel technologies in 5G networks. Current channel models such as WINNER+ have some limitations. For example, although the WINNER is an antenna independent model, its implementation is now only applicable to uniform linear arrays [26]. New 3-D models need to support massive and ultradense antenna deployments, greater bandwidth, higher carrier frequencies, high-speed users, new deployment scenarios such as D2D communication, and transitions between different propagation environments (e.g., urban, rural, outdoor, or indoor).

ANTENNA ARRAY DESIGN

As mentioned before, the antenna at a BS of cellular systems is usually implemented as a linear array of a limited number of antennas in the azimuth plane. However, these geometries can shape the radiation pattern only in the horizontal plane, and hence to change the beam in the elevation plane for 3DBF, more general 2-D or 3-D arrays topologies are necessary. Those arrays are active antenna systems that are spaced in both azimuth and vertical planes with different configurations such as planar, circular, spherical, or cylindrical structures. In addition, the array may include copolarized or cross-polarized antenna elements. The active antenna arrays placed in 2-D are also called full-dimension MIMO (FD-MIMO) or 3-D MIMO [27]. Massive MIMO, which employs up to several hundreds of antenna elements, can be a potential extension of 3DBF for 5G systems.

In general, adding more antenna elements to the array provides more flexibility in beam steering designs and increases the number of radiation beams of the array. For vertical sectorization in which the number of vertical sectors is usually small (e.g., two or three), only a small number of antennas are required in the vertical plane. However, in 3DBF with per-user beam pattern adaptation (i.e., user tracking), a large number of antennas are needed. Hence, one of the challenges of the 3DBF is physical constraints and placement of a large number of antennas at a BS. This problem may be alleviated in higher frequencies that are expected for 5G networks. Also FD-MIMO can be utilized to address this issue. For example, in [27] a 2-D array of 32 antennas comprising eight antenna ports in the horizontal plane and four antenna ports in

the vertical dimension is proposed. Each antenna port consists of a sub-array of four antennas in the vertical dimension, which results in a total of 128 elements in this antenna. The size of this antenna in the 2.5 GHz band is 1 m × 0.5 m, which is appropriate to fit on a BS tower. A similar study shows that the same number of antennas can be placed on a cylinder with a diameter of 1 m [28]. Another challenge of adding more antenna elements at the BS is cost related to RF chains required for all antennas, which needs to be addressed in future research.

One more important factor in the BS antenna design is the pattern shape of the array. A desired pattern in the 3-D space can be determined by methods such as the Fourier–Bessel series [29]. Most of these pattern synthesis techniques were proposed for planar arrays and symmetric arrays such as circular arrays. Their aim is to determine the main-lobe shape and side-lobe levels. Besides, most of the beam pattern designs (or array design methods) are based on narrowband systems, which are not appropriate for next-generation wireless systems. Hence, it is important to consider more advanced array configurations and wideband beam shaping designs. Generally, to widen the bandwidth of the arrays, different structures in different frequencies can be employed. It is also possible to apply frequency invariant antenna arrays [29].

In the model introduced by the ITU [20], the antenna radiation pattern in a given user's direction is defined by

$$A_P(\theta, \phi) = G_{\max} - \min\{A_H(\theta) + A_V(\phi), A_m\}, \quad (1)$$

where G_{\max} , θ , and ϕ denote the maximum antenna gain at the main beam (boresight) direction, the angles of the user direction from the boresight direction in the horizontal plane, and the tilting angle of the user, respectively, as shown in Figure 6. Here A_H and A_V stand for the relative antenna gains in the horizontal and vertical planes, respectively, expressed as

$$A_H(\theta) = \min\left[12\left(\frac{\theta}{\theta_{3\text{dB}}}\right)^2, A_m\right] \quad (2)$$

$$A_V(\phi) = \min\left[12\left(\frac{\phi - \phi_{\text{tilt}}}{\phi_{3\text{dB}}}\right)^2, A_m\right], \quad (3)$$

where ϕ_{tilt} represents the main beam tilting angle, $\theta_{3\text{dB}}$ and $\phi_{3\text{dB}}$ indicate the 3-dB beamwidth of the horizontal and vertical patterns, respectively, and A_m equals the side-lobe level attenuation of the antenna pattern. In normal situations, we usually have $A_m = 20\sim 30$ dB, $\theta_{3\text{dB}} = 60^\circ\sim 70^\circ$, and $\phi_{3\text{dB}} = 8^\circ\sim 15^\circ$.

SIMULATION RESULTS

In this section, we present the efficiency of the 3DBF compared to the 2DBF through Monte Carlo simulation. For simulations, we adopt the WINNER+ channel model and the urban microcell environment in [20] and [25] with slight modifications. We assume that a single user is active per sector at each time slot. Also, users are uniformly distributed in all cells, and the BS has

THROUGH NUMERICAL SIMULATIONS, IT IS SHOWN THAT THE 3DBF OUTPERFORMS THE CONVENTIONAL 2DBF, AND THUS IT IS EXPECTED THAT 3DBF WILL PLAY A CRUCIAL ROLE IN 5G SYSTEM DESIGNS.

perfect CSI to compute transmit precoding vectors. Table 1 illustrates the simulation settings. We assume that the BS antenna structure is the uniform linear array with 10λ antenna spacing where λ denotes the wavelength of the system. The 2DBF is evaluated by the horizontal gain in (2). In these simulations, for the case of the dynamic 3DBF, the

tilting angle ϕ_{tilt} is set to the actual vertical angle of the user ϕ . This means that the vertical beam pattern is adapted to the user locations in a dynamic way. We also present the performance of

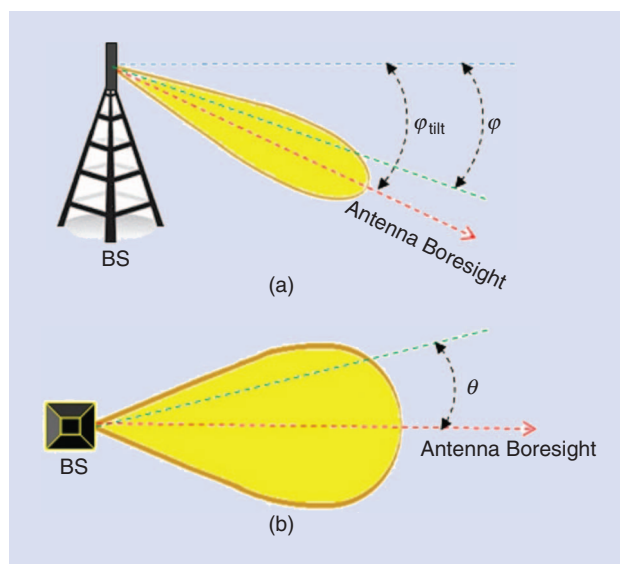


[FIG6] Three-dimensional antenna pattern modeling (a) the vertical plane and (b) the horizontal plane.

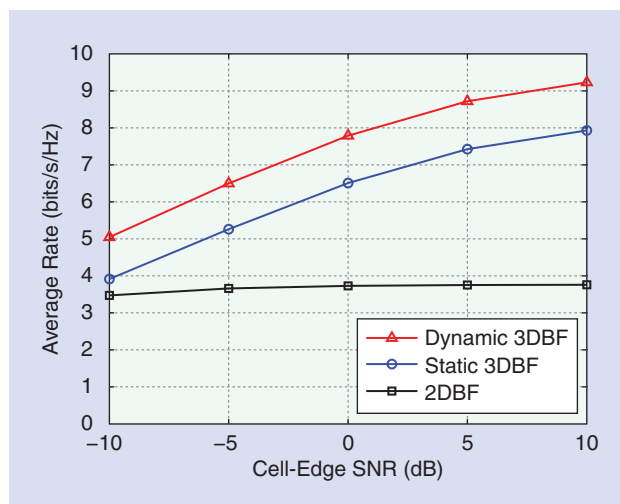


[FIG7] The average rate performance comparison as a function of cell-edge SNR.

[TABLE 1] THE SIMULATION SETTINGS.

CELL TYPE	URBAN MICRO
CELL LAYOUT	SEVEN CELLS WITH THREE SECTORS PER CELL
INTERSITE DISTANCE	200 m
CHANNEL MODEL	WINNER+
MINIMUM DISTANCE BETWEEN A USER AND A BS	10 m
NUMBER OF Tx ANTENNAS AT BS	4
NUMBER OF Rx ANTENNAS OF A USER	1
SCHEDULER	ROUND-ROBIN
TRANSMIT PRECODING	MAXIMAL RATIO TRANSMISSION
BS ANTENNA HEIGHT	10 m
USER ANTENNA HEIGHT	1.5 m
PATH LOSS EXPONENT	3.4
MAXIMUM ANTENNA GAIN	17 dB
MAXIMUM ATTENUATION OF THE BS ANTENNA	20 dB
VERTICAL 3-dB BEAMWIDTH	8°
HORIZONTAL 3-dB BEAMWIDTH	65°

the static 3-D where the tilting angle is fixed. In this case, the optimal tilting angle ϕ_{tilt}^* is obtained from exhaustive search.

Figure 7 exhibits the average rate performance with respect to the cell-edge signal-to-noise ratio (SNR), which is defined as the received SNR at the cell boundary. Compared to the 2DBF, the average rate is enhanced by 75% in the static 3DBF with the fixed tilting angle $\phi_{\text{tilt}}^* = 11^\circ$ when the cell-edge SNR is equal to 0 dB. These performance improvements are due to a reduction of intercell interference that results from narrow vertical beam adjustment. Also, the dynamic 3DBF achieves a performance gain of 109% over the 2DBF at the cell-edge SNR of 0 dB. We can see that the dynamic 3DBF outperforms the static 3DBF, since the vertical beam in the dynamic beamforming can be adaptively aligned to the user position. This performance gap between the 3DBF and the 2DBF increases as the cell-edge SNR grows.

To illustrate the effect of the vertical 3-dB beamwidth of the BS antennas on the performance, Figure 8 presents the average rate of the 3DBF and the 2DBF for different $\phi_{3\text{dB}}$ when the cell-edge SNR is

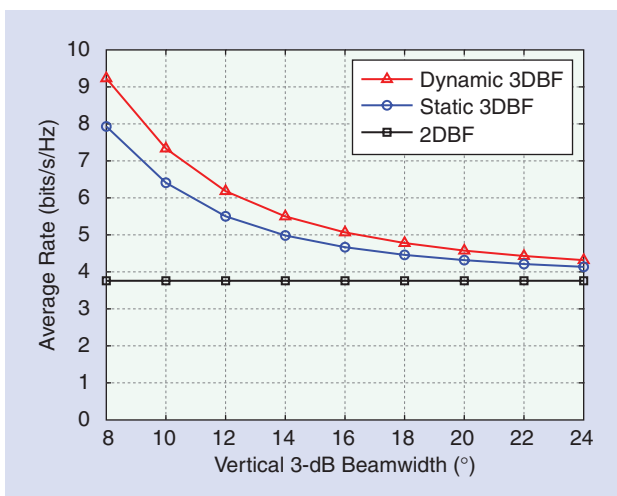


[FIG8] The average rate performance comparison as a function of vertical 3-dB beamwidth.

set to 10 dB. Since the 2DBF is not affected by the vertical 3-dB beamwidth, the average rate performance remains constant. However, the performance gain of the 3DBF compared to the 2DBF grows as the antenna vertical beamwidth becomes smaller, since a larger vertical 3-dB beamwidth results in more intercell interference.

We also compare vertical sectorization with the conventional horizontal sectorization. In this case, the vertical sectorization is evaluated by adopting two fixed tilting angles $\phi_{\text{tilt}1}$ and $\phi_{\text{tilt}2}$ in the cell. In a similar manner as the static 3DBF case, the optimum tilting angles for the vertical sectorization can be found by the exhaustive search method. For a fair comparison, we assume that each beam power of the vertical sectorization is the half of that of the conventional case. Figure 9 shows the average rates of the conventional sectorization with $\phi_{\text{tilt}}^* = 11^\circ$ and the vertical sectorization with $\phi_{\text{tilt}1}^* = 25^\circ, \phi_{\text{tilt}2}^* = 11^\circ$, respectively. It is observed that the vertical sectorization leads to an average rate performance gain of 124% compared to the conventional sectorization at the cell-edge SNR of 0 dB. In summary, throughout the simulations, we can see that the 3DBF is able to reduce intercell interference and improve the average sum rate, and thus it brings out a significant performance gain over 2DBF. This makes the 3DBF as a promising technology for 5G systems.

CONCLUSIONS

In this article, we have investigated the 3DBF as a candidate technique that enables 5G wireless systems. In the 3DBF, the radiation beam pattern is adapted in both an elevation and horizontal plane that provides more degrees of freedom in system designs. Compared to the 2DBF, the 3DBF has many advantages including higher user capacity and less intercell and intersector interference. By employing the 3-D antenna pattern modeling, we have evaluated Monte Carlo simulation and then provided the performance comparison between the 3DBF and the 2DBF. Through numerical simulations, it is shown that the 3DBF outperforms the conventional 2DBF, and thus it is expected that 3DBF will play a crucial role in 5G system designs.

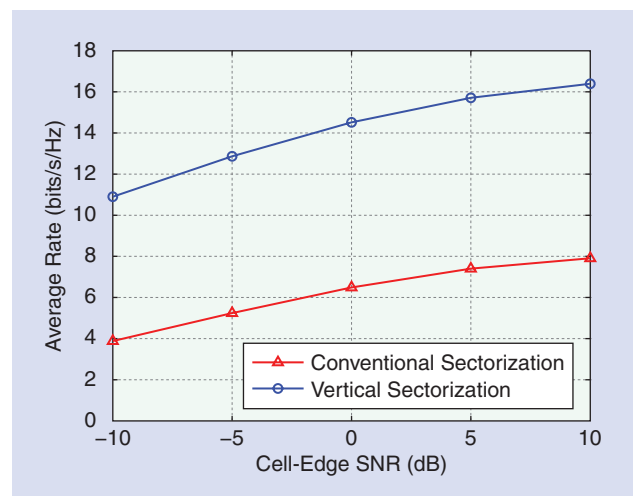


[FIG9] The average rate performance comparison as a function of cell-edge SNR.

AUTHORS

S. Mohammad Razavizadeh (smrazavi@iust.ac.ir) received his B.Sc., M.Sc., and Ph.D. degrees from the Iran University of Science and Technology (IUST), Tehran, Iran, in 1997, 2000, and 2006, respectively, all in electrical engineering. From June 2004 to April 2005, he was a visiting scholar with Coding and Signal Transmission Laboratory, University of Waterloo, Ontario, Canada. From 2005 to 2011, he was with Iran Telecommunication Research Center, Tehran, as a research assistant professor. Since 2011, he has been with the Department of Electrical Engineering at IUST, where he is currently an assistant professor. During the summer of 2013, he was with the Wireless Communications Laboratory at Korea University, Seoul, South Korea, as a visiting professor. His research interests are in the area of signal processing for wireless communication systems and cellular networks. He is a Senior Member of the IEEE.

Minki Ahn (amk200@korea.ac.kr) received the B.S. and M.S. degrees in electrical engineering from Korea University, Seoul, South Korea, in 2010 and 2012, where he is currently working toward the Ph.D. degree in the School of Electrical Engineering. During the winter of 2011, he was a visiting student at the Queen's University, Kingston, Ontario, Canada. His research interests include information theory and signal processing for wireless communication systems, such as the relay network, three-dimensional beamforming, and the multicell network.

Inkyu Lee (inkyu@korea.ac.kr) received the B.S. degree in control and instrumentation engineering from Seoul National University, South Korea, in 1990, and the M.S. and Ph.D. degrees in electrical engineering from Stanford University, California, in 1992 and 1995, respectively. He is currently a professor in the School of Electrical Engineering, Korea University, Seoul, South Korea. He has published over 110 journal papers with the IEEE, and has 30 U.S. patents granted or pending. His research interests include digital communications and signal processing techniques applied for next-generation wireless systems. He has served as an associate editor of *IEEE Transactions on Communications* and *IEEE Transactions on Wireless Communications*. He was a chief guest editor of *IEEE Journal on Selected Areas in Communications* (Special Issue on 4G Wireless Systems) in 2006. He received numerous awards including the Best Young Engineer Award of the National Academy of Engineering of Korea in 2013.

REFERENCES

- [1] 3GPP, "Report of 3GPP RAN Workshop on Release 12 and onwards," RWS-120052, 3GPP Workshop on Release 12 Onward, June 2012.
- [2] 3GPP, "Requirements, Candidate Solutions and Technology Roadmap for LTE Rel-12 Onward," RWS-120010, 3GPP Workshop on Release 12 Onward, June 2012.
- [3] D. Gesbert, M. Kountouris, R. W. Heath, Jr., C. B. Chae, and T. Salzer, "From single user to multiuser communications: Shifting the MIMO paradigm," *IEEE Signal Processing Mag.*, vol. 24, no. 5, pp. 36–46, Oct. 2007.
- [4] H. Sung, S.-R. Lee, and I. Lee, "Generalized channel inversion methods for multiuser MIMO systems," *IEEE Trans. Commun.*, vol. 57, no. 5, pp. 3489–3499, Nov. 2009.
- [5] H. Lee, B. Lee, and I. Lee, "Iterative detection and decoding with an improved V-BLAST for MIMO-OFDM systems," *IEEE J. Select. Areas Commun.*, vol. 24, pp. 504–513, Mar. 2006.
- [6] 3GPP, "Text proposal on mechanical and electrical antenna tilting," Tech. Rep. RI-135708, Fraunhofer IIS, 3GPP RAN WG1 Meeting no. 75, Nov. 2011.

- [7] W. Lee, S. R. Lee, H. B. Kong, and I. Lee, "3D beamforming designs for single user MISO systems," in *Proc. IEEE Global Communications Conf.*, Dec. 2013, pp. 3914–3919.
- [8] H. Huang, O. Alrabadi, J. Daly, D. Samardzija, C. Tran, R. Valenzuela, and S. Walker, "Increasing throughput in cellular networks with higher-order sectorization," in *Proc. Asilomar Conf. Signals, Systems and Computers*, Nov. 2010, pp. 630–635.
- [9] C. S. Lee, M. C. Lee, C. J. Huang, and T. S. Lee, "Sectorization with beam pattern design using 3D beamforming techniques," in *Proc. Asia-Pacific Signal and Information Processing Association Annual Summit and Conf.*, Oct. 2013, pp. 1–5.
- [10] P. Kang, Q. Cui, S. Chen, and Y. Liu, "Performance evaluation on coexistence of LTE with active antenna array systems," in *Proc. IEEE Int. Symp. Personal Indoor and Mobile Radio Communications*, Sept. 2012, pp. 1066–1070.
- [11] A. Adhikary, J. Nam, J. Ahn, and G. Caire, "Joint spatial division and multiplexing—The large-scale array regime," *IEEE Trans. Inform. Theory*, vol. 59, no. 10, pp. 6441–6463, Oct. 2013.
- [12] T. L. Marzetta, "How much training is required for multiuser MIMO?," in *Proc. Asilomar Conf. Signals, Systems and Computers*, Oct./Nov. 2006, pp. 359–363.
- [13] H. E. Lee, "Synthetic array processing for underwater mapping applications," in *Proc. IEEE Int. Conf. Acoustics, Speech, and Signal Processing*, Aug. 1978, pp. 148–151.
- [14] M. Karaman, I. O. Wygant, O. Oralkan, and B. T. Khuri-Yakub, "Minimally redundant 2-D array designs for 3-D medical ultrasound imaging," *IEEE Trans. Med. Imaging*, vol. 28, no. 7, pp. 1051–1061, July 2009.
- [15] A. C. Dhanantwari, S. Stergiopoulos, L. Song, C. Parodi, F. Bertora, P. Pellegretti, and A. Questa, "An efficient 3D beamformer implementation for real-time 4D ultrasound systems deploying planar array probes," in *Proc. IEEE Ultrasonics Symp.*, Aug. 2004, vol. 2, pp. 1421–1424.
- [16] J. M. Valin, F. Michaud, and J. Rouat, "Robust 3D localization and tracking of sound sources using beamforming and particle filtering," in *Proc. IEEE Int. Conf. Acoustics, Speech and Signal Processing*, May 2006, pp. 841–844.
- [17] J. Meyer and G. Elko, "A highly scalable spherical microphone array based on an orthonormal decomposition of the soundfield," in *Proc. IEEE Int. Conf. Acoustics, Speech, and Signal Processing*, May 2002, vol. 2, pp. 1781–1784.
- [18] H. Kanj, P. Lusina, S. M. Ali, and F. Kohandani, "A 3D-to-2D transform algorithm for incorporating 3D antenna radiation patterns in 2D channel simulators," *IEEE Antenna Propagat. Wireless Lett.*, vol. 8, pp. 815–818, June 2009.
- [19] 3GPP, "Spatial channel model for multiple input multiple output (MIMO) simulations (Release 9)," 3GPP, Tech. Rep. TR 25.996 V9.0.0, Dec. 2009.
- [20] ITU-R Report M.2135-1, "Guidelines for evaluation of radio interface technologies for IMT-advanced," 2009.
- [21] R. H. Clarke, "A statistical theory of mobile radio reception," *Bell Syst. Tech. J.*, vol. 47, pp. 957–1000, July/Aug. 1968.
- [22] A. Kuchar, J.-P. Rossi, and E. Bonek, "Directional macro-cell channel characterization from urban measurements," *IEEE Trans. Antennas Propagat.*, vol. 48, no. 2, pp. 137–146, Feb. 2000.
- [23] 3GPP, "Study on 3D channel model for LTE (Release 12)," Tech. Rep. RI-134980, Sept. 2013.
- [24] T. Aulin, "A modified model for the fading signal at a mobile radio channel," *IEEE Trans. Veh. Technol.*, vol. 28, no. 3, pp. 182–203, Aug. 1979.
- [25] J. Meinila, P. Kyosti, L. Hentila, T. Jamsa, E. Suikkanen, E. Kunnari, and M. Narandzic, "D5.3: WINNER+ final channel models," in *Wireless World Initiative New Radio—WINNER+*, P. Heino, Ed., CELTIC/CP5-026, 2010.
- [26] M. Narandzic, C. Schneider, R. S. Thoma, T. Jamsa, P. Kyosti, and X. Zhao, "Comparison of SCM, SCME, and WINNER channel models," in *Proc. IEEE Vehicular Technology Conf.*, Apr. 2007, pp. 413–417.
- [27] Y. H. Nam, B. L. Ng, K. Sayana, Y. Li, J. Zhang, Y. Kim, and J. Lee, "Full-dimension MIMO (FD-MIMO) for next-generation cellular technology," *IEEE Commun. Mag.*, vol. 51, no. 6, pp. 172–179, June 2013.
- [28] E. Larsson, O. Edfors, F. Tufvesson, and T. Marzetta, "Massive MIMO for next-generation wireless systems," *IEEE Commun. Mag.*, vol. 52, no. 2, pp. 186–195, Feb. 2014.
- [29] Y. Li, K. C. Ho, and C. Kwan, "3-D array pattern synthesis with frequency invariant property for concentric ring array," *IEEE Trans. Signal Processing*, vol. 54, no. 2, pp. 780–784, Feb. 2006.
- [30] F. Zotter and B. Bank, "Geometric error estimation and compensation in compact spherical loudspeaker array calibration," in *Proc. IEEE Int. Instrumentation and Measurement Technology Conf.*, pp. 2710–2715, May 2012.